49th IEEE Conference on Decision and Control
December 15-17, 2010
Hilton Atlanta Hotel, Atlanta, GA, USA

Probabilistic 4D Trajectory Prediction and Conflict Detection for Air Traffic Control

Weiyi Liu and Inseok Hwang

Abstract— **In this paper, we study the problem of aircraft 4D trajectory prediction and conflict detection which is one of the key functions of the Next Generation Air Transportation System (NextGen). A stochastic linear hybrid system (SLHS) with two different discrete state transition models is proposed to describe the aircraft motion. Based on the SLHS model, a 4D trajectory prediction algorithm is proposed utilizing some prior information about the aircraft's intent. Also, a computationally efficient conflict detection algorithm is developed based on the cumulative distribution function (cdf) approximation for the quadratic form of Gaussian random variables. The performance of the proposed algorithms is validated through an illustrative air traffic scenario.**

I. INTRODUCTION

In this paper, we study the problem of 4D aircraft trajectory prediction and conflict detection which is one of the key functions of the Next Generation Air Transportation System (NextGen)[1]. Aircraft trajectory prediction involves estimating an aircraft's future trajectory by using the measurements up to the current time. Based on the trajectory prediction results, the corresponding conflict detection algorithm makes a decision (or calculates the probabilities) whether there will be a potential conflict in the predicted time span [2]. Typically, methods to solve these two problems can be categorized into three kinds: nominal, worst case and probabilistic [3]. The probabilistic method predicts the aircraft trajectory by propagating the probability density function (pdf) of its position into the future and computes the probability of conflict. The probabilistic approach is useful because (a) it is more appropriate to model the aircraft motion by using a stochastic model due to various uncertainties such as wind gust, navigational error, etc.; and (b) it enables us to assess the conflict probability and set different thresholds to declare a conflict in different scenarios.

The proposed algorithm is based on the probabilistic approach. Before our work, Lygeros et. al. proposed probabilistic aircraft and weather models for the purpose of collision avoidance [4]. For computational simplicity, Paielli et. al. approximated the conflict probability by using a stripe to replace the circular protection zone [5]. Yang et. al. proposed an algorithm based on the Monte Carlo method [6]. Hu et. al. used Markov Chain to approximate the solution of stochastic differential equations which describes aircraft motion [7]. The work in this paper is based on our previous research [2]. The stochastic linear hybrid system (SLHS) model is applied to describing the aircraft motion. This model incorporates a multiple model set in which each individual model captures one flight mode of an aircraft. In NextGen, aircraft's intent will be available through ADS-B [1]. To incorporate this information into our model, the stochastic guard conditions are used to model the flight mode transition. To evaluate the conflict probability, we propose a conflict detection algorithm. As the distance (which is a random variable) between two aircraft can be written in the quadratic form of Gaussian random variables, we can use the Laurent series expansion to approximate its cumulative distribution function (cdf), thereby evaluating the conflict probabilities computationally efficiently. To demonstrate the performance of our algorithm, we apply it to a two-aircraft trajectory prediction and conflict detection scenario.

The rest of the paper is organized as follows: In Section II, the SLHS model is briefly reviewed. Based on the SLHS model, the problem of trajectory prediction and conflict detection is mathematically formulated. The probabilistic trajectory prediction algorithms and the conflict detection algorithm are presented in Section III. Section IV demonstrates the performance of our algorithm through a two-aircraft conflict scenario. Conclusions are given in Section V.

II. MATHEMATICAL FORMULATION OF THE TRAJECTORY PREDICTION AND CONFLICT DETECTION PROBLEMS

In this section, we first review the Stochastic Linear Hybrid System (SLHS) model. Then the problem of trajectory prediction and conflict detection is mathematically formulated.

A. Hybrid System Model

The SLHS model contains several continuous models (discrete states), each matched to a flight mode. The continuous state dynamics in each mode are described by the following difference equations:

$$x(k) = A_{q(k)}x(k-1) + B_{q(k)}w(k) \quad (1)$$

where $x(k) \in \mathscr{X} = \mathbb{R}^n$ is the state vector; $q(k) \in \mathscr{Q} = \{1, 2, \ldots, n_d\}$ is the discrete state at time k; $\mathscr{Q}$ is a finite set of all the discrete states; A_q and B_q are the system matrices with appropriate dimensions, corresponding to each discrete state $q \in \mathscr{Q}$; and $w(k) \in \mathbb{R}^p$ is the white Gaussian process noise with zero mean and covariance $Q(k)$.

There are two types of discrete state (mode) transitions in the SLHS:

1) *Markov-jump transition model*: The finite state space of the Markov Chain is the discrete state space $\mathscr{Q}$.

Authors are with the School of Aeronautics and Astronautics, Purdue University, West Lafayette, IN, 47907 USA `liu61@purdue.edu`, `ihwang@purdue.edu`

Suppose at each time k, the probability vector is given by $\pi(k) = \left[\pi_1(k)\cdots\pi_{n_d}(k)\right]^T$, with each entry of the vector ($\pi_i(k)$) denotes the probability that the system's true discrete state is i. Then, at the next time step the probability vector is:

$$\pi(k+1) = \Gamma\pi(k) \quad (2)$$

where a constant matrix Γ is the Markov transition matrix.

2) *State-dependent transition model*: the discrete state transition is governed by:

$$q(k+1) = \gamma(q(k), x(k), \theta) \quad (3)$$

where $\theta \in \Theta = \mathbb{R}^l$ and $\gamma : \mathscr{Q} \times \mathscr{X} \times \Theta \to \mathscr{Q}$ is the *discrete-state transition function* defined as:

$$\gamma(i, x, \theta) = j \quad \text{if } [x^T \ \theta^T]^T \in G(i, j)$$

$G(i, j)$ is called as the *guard condition*. For each combination of (i, j), the guard condition $G(i, j)$ is a subset of the space $\Omega = \mathscr{X} \times \Theta$ with the following assumption:

Assumption 1: The set of guards $\{G(i, j)|j \in \mathscr{Q}\}$ is a partition of the space Ω for any given $i \in \mathscr{Q}$:

$$G(i, j) \cap G(i, k) = \phi \qquad \forall i, j, k \in \mathscr{Q} \text{ and } j \neq k, \quad (4)$$

and

$$\bigcup_{j=1}^{r} G(i, j) = \Omega \qquad \forall i \in \mathscr{Q} \quad (5)$$

In this paper, we consider a specific kind of the guard condition $\{G(i, j)|i, j \in \mathscr{Q}\}$ named as the *stochastic linear guard condition*:

$$G(i, j) = \left\{ \begin{bmatrix} x \\ \theta \end{bmatrix} \middle| x \in X, \theta \in \Theta, L_{ij} \begin{bmatrix} x \\ \theta \end{bmatrix} + b_{ij} \leq 0 \right\} \quad (6)$$

where $\theta \in \Theta = \mathbb{R}^l$ and $\theta \sim \mathscr{N}_l(\theta; \bar{\theta}, \Sigma_\theta)$ is a l-dimensional Gaussian random vector with mean $\bar{\theta}$ and covariance Σ_θ representing uncertainties in the guard condition; L_{ij} is a $\zeta \times (n+l)$ matrix, b_{ij} is a constant ζ-dimensional vector, and ζ is the dimension of the vector inequality. Here, a vector inequality $y \leq 0$ means that each scalar element of y is non-positive. In this model, the dependency of the mode transition on the continuous state models the aircraft's intent or flight plan, while the random variable θ models the uncertainties in the mode transition.

B. Problem Formulation

Consider M aircraft $\{a_m|m = 1, \ldots, M\}$ flying in the 3-D airspace $\mathscr{S} \subset \mathbb{R}^3$ during the look-ahead time horizon $T = [k_c T_s, (k_c + k_p)T_s]$ where T_s is the sampling interval; k_c and k_p are the current time step and the look-ahead time step. Let (ξ, η, h) be the coordinates of an aircraft in the local navigation frame with ξ-axis pointing the east, η-axis pointing the north and h-axis pointing up. Thus, the state of each aircraft is defined as $x = [\xi \ \dot{\xi} \ \eta \ \dot{\eta} \ h \ \dot{h}]^T \in \mathscr{X} = \mathscr{R}^6$. In the time horizon T, each aircraft's continuous state $x^{a_m}(k)$ evolves according to the continuous dynamics (1), while its discrete state $q^{a_m}(k)$ evolves according to the following rule: if the information about the aircraft's intent (e.g. waypoint information, landing profile information, etc.) is available, the flight mode transition is modeled by the discrete dynamics in (3); otherwise, it is modeled by the Markov transition in (2) [8]. Before the time step k_c, the hybrid estimation algorithm [9] computes the probability mass function (pmf) of the flight mode $p[q^{a_m}(k)]$[1], and the pdf of the current state which are given by:

$$\begin{aligned} p[x^{a_m}(k)] &= \sum_{i \in \mathscr{Q}} p[x^{a_m}(k)|q^{a_m}(k) = i] Pr\{q^{a_m}(k) = i\} \\ &\approx \sum_{i \in \mathscr{Q}} \mathscr{N}_6(x^{a_m}(k); \hat{x}_i^{a_m}(k), P_i^{a_m}(k)) Pr\{q^{a_m}(k) = i\} \quad (7) \\ &\approx \mathscr{N}_6(x^{a_m}(k); \hat{x}^{a_m}(k), P_x^{a_m}(k)) \quad k \leq k_c \end{aligned}$$

Note that in (7), a single Gaussian random variable is used to approximate the sum of several Gaussian random variables via moment matching [8]. Based on the estimation result up to time k_c, the trajectory prediction algorithm computes the pmf of the discrete state $p[q^{a_m}(k)]$ and the pdf of the continuous state conditioned on different discrete states $p[x^{a_m}(k)|q^{a_m}(k) = i]$, for all $k \in [k_c, k_c + k_p]$. The 4D predicted trajectory can be computed by:

$$\begin{aligned} p[z^{a_m}(k)] &= \mathscr{N}_3(z^{a_m}(k); \hat{z}^{a_m}(k), P_z^{a_m}(k)) \\ &= \mathscr{N}_3(z^{a_m}(k); C\hat{x}^{a_m}(k), CP_x^{a_m}(k)C^T) \end{aligned} \quad (8)$$

where

$$C = \begin{bmatrix} 1 & 0 & 0 & 0 & 0 & 0 \\ 0 & 0 & 1 & 0 & 0 & 0 \\ 0 & 0 & 0 & 0 & 1 & 0 \end{bmatrix}$$

Next, the problem of conflict detection is presented. Consider a scenario where there are two aircraft a_1 and a_2 in the region $\mathscr{S}$. We fix one aircraft (reference aircraft) at the origin and study the motion of the other aircraft (stochastic aircraft) in the relative frame. A midair conflict is thus defined as the event that the stochastic aircraft enters the protected zone of the reference aircraft. Rather than the cylindrical protected zone [5], we consider the protected zone in the quadratic form (ellipsoid) [10]. Our method can be easily extended to the cylindrical protected zone case. The quadratic protected zone can be represented as:

$$\mathscr{D} = \left\{ (\xi_r, \eta_r, h_r) \middle| \left(\frac{\xi_r}{s}\right)^2 + \left(\frac{\eta_r}{s}\right)^2 + \left(\frac{h_r}{H}\right)^2 \leq 1 \right\} \quad (9)$$

where s and H are the radii of the protected zone in the horizontal plane and the vertical dimension, respectively; ξ_r, η_r and h_r are the relative position of the stochastic aircraft with respect to the reference aircraft. Let $\rho_{12}(k) = z^{a_1}(k) - z^{a_2}(k)$ be the relative distance between aircraft a_1 and a_2 in the (ξ_r, η_r, h_r) frame. Assuming the two aircraft's motions are independent, the pdf of ρ_{12} can be written as:

$$\begin{aligned} p[\rho_{12}(k)] &= \mathscr{N}_3(\rho_{12}(k); \bar{\rho}_{12}(k), \Sigma_{12}(k)) \\ \bar{\rho}_{12}(k) &= \hat{z}^{a_1}(k) - \hat{z}^{a_2}(k), \\ \Sigma_{12}(k) &= P_z^{a_1}(k) + P_z^{a_2}(k) \end{aligned}$$

[1]Throughout this paper, we use $Pr\{\bullet\}$ to denote the probability of an event and $p[\bullet]$ for the pdf or pmf.

Then, the conflict probability over the time horizon T is defined as:

$$Pr\{\mathscr{C}|T\} := \max_{k\in[k_c,k_c+k_p]} Pr\{\mathscr{C}(k)\}$$

where $Pr\{\mathscr{C}(k)\}$ is the *instantaneous* probability of conflict at time k given by:

$$Pr\{\mathscr{C}(k)\} = \int_{\rho\in\mathscr{D}} \mathscr{N}_3(\rho;\bar{\rho}_{12}(k);\Sigma_{12}(k))d\rho \qquad (10)$$

III. PROBABILISTIC TRAJECTORY PREDICTION AND CONFLICT DETECTION ALGORITHMS

In this section, we derive the trajectory prediction algorithm and the conflict detection algorithm.

A. Trajectory Prediction Algorithm

Assuming the aircraft dynamics is given by (1) combined with (2) or (3), the trajectory prediction algorithm is based on a multiple-model set in which each model is matched to an aircraft's flight mode. In the following part of this paper, for simplicity, we ignore the superscript a_n in x^{a_n}, q^{a_n} and other variables for a specific aircraft a_n in the region $\mathscr{S}$. Our algorithm is composed of 4 steps:

- **Step 1. Initialization:** We use $\mathscr{Z}^{k_c}$ to denote the observations (measurements) up to time k_c. From the hybrid estimation algorithm, we have both the current continuous state pdf conditioned on each discrete state, $p[x(k_c)|q(k_c)=i,\mathscr{Z}^{k_c}] = \mathscr{N}_n(x(k_c);\hat{x}_i(k_c),P_i(k_c))$ and the current discrete state pmf, $p[q(k_c)|\mathscr{Z}^{k_c}]$.
- **Step 2. Compute mixing (merging) probabilities:** The mixing probabilities $Pr\{q(k)=i|q(k+1)=j,\mathscr{Z}^{k_c}\}$ for all $i,j\in\mathscr{Q}$ are defined as:

  $$\mu_{ji}(k) := Pr\{q(k)=i|q(k+1)=j,\mathscr{Z}^{k_c}\} \qquad (11)$$

  By Bayes' Theorem,

  $$\begin{aligned}&Pr\{q(k)=i|q(k+1)=j,\mathscr{Z}^{k_c}\} = \\ &\frac{1}{c_j}Pr\{q(k+1)=j|q(k)=i,\mathscr{Z}^{k_c}\}p\left[q(k)|\mathscr{Z}^{k_c}\right]\end{aligned} \qquad (12)$$

  where c_j is a normalizing constant. For (11) and (12), we use the following approach to compute the discrete state transition probability $Pr\{q(k+1)=j|q(k)=i,\mathscr{Z}^{k_c}\}$:

  1) *Markov-jump transition*: the Markov transition matrix provides the *a priori* knowledge directly. The discrete state transition probability $Pr\{q(k+1)=j|q(k)=i,\mathscr{Z}^{k_c}\}$ in (12) can be written as:

  $$Pr\{q(k+1)=j|q(k)=i,\mathscr{Z}^{k_c}\} = \Gamma_{ij} = const. \qquad (13)$$

  2) *State-dependent transition*: we recall that $\theta\in\Theta=\mathbb{R}^l \sim \mathscr{N}_l(\theta;\bar{\theta},\Sigma_\theta)$ has a multivariate Gaussian distribution (if $\Theta\neq\emptyset$). With the stochastic linear guard condition given in (6), we compute the discrete state transition probability $Pr\{q(k+1)=j|q(k)=i,\mathscr{Z}^{k_c}\}$ in (12) as [9]:

  $$\begin{aligned}&Pr\{q(k+1)=j|q(k)=i,\mathscr{Z}^{k_c}\}\\ &=\Phi_\zeta\left(L_{ij}\begin{bmatrix}\hat{x}_i(k)\\ \theta\end{bmatrix}+b_{ij},L_{ij}\begin{bmatrix}P_i(k) & 0\\ 0 & \Sigma_\theta\end{bmatrix}L_{ij}^T\right)\end{aligned} \qquad (14)$$

  where $\Phi_\zeta(\bar{y},\Sigma_y)$ is the ζ-dimensional Gaussian cdf with mean $\bar{y}$ and covariance Σ_y.
- **Step 3. Update pdf:** By the totoal probability theorem,

  $$\begin{aligned}&p[x(k+1)|q(k+1)=j,\mathscr{Z}^{k_c}] = \sum_{i\in\mathscr{Q}}\\ &p[x(k+1)|q(k+1)=j,q(k)=i,\mathscr{Z}^{k_c}]Pr\{q(k)=i|\mathscr{Z}^{k_c}\}\end{aligned} \qquad (15)$$

  To evaluate (15), we need to compute n_d^2 pdfs $p[x(k+1)|q(k+1)=j,q(k)=i,\mathscr{Z}^{k_c}]$ for $i,j=1,2,\dots,n_d$. To reduce the computational complexity, we assume each pdf $p[x(k+1)|q(k+1)=j,q(k)=i,\mathscr{Z}^{k_c}]$ to be Gaussian and approximate (15) by a single Gaussian pdf via moment matching [11]:

  $$\begin{aligned}&p[x(k+1)|q(k+1)=j,\mathscr{Z}^{k_c}] =\\ &\qquad \mathscr{N}_n(x(k+1);\hat{x}_j(k+1),P_j(k+1))\end{aligned} \qquad (16)$$

  where

  $$\hat{x}_j(k+1) = A_j\hat{x}_{j0}(k) \qquad (17)$$

  $$P_j(k+1) = A_jP_{j0}(k)A_j^T + B_jQ_jB_j^T \qquad (18)$$

  $$\hat{x}_{j0}(k) = \sum_{i=1}^{n_d}\mu_{ji}(k)\hat{x}_i(k) \qquad (19)$$

  $$\begin{aligned}P_{j0}(k) = &\sum_{i=1}^{n_d}\mu_{ji}(k)\{P_i(k)\\ &+[\hat{x}_i(k)-\hat{x}_{j0}(k)][\hat{x}_i(k)-\hat{x}_{j0}(k)]^T\}\end{aligned} \qquad (20)$$

  The discrete state probability at time $k+1$ is given by

  $$\begin{aligned}Pr\{q(k+1)=j|\mathscr{Z}^{k_c}\} &:= \alpha_j(k+1)\\ &=\sum_{i=1}^{n_d}Pr\{q(k+1)=j|q(k)=i,\mathscr{Z}^{k_c}\}\alpha_i(k)\end{aligned}$$
- **Step 4. Output:** The discrete state estimates are given by:

  $$\hat{q}(k+1) = \max_j Pr\left\{q(k+1)=j|\mathscr{Z}^{k_c}\right\}$$

  By the total probability theorem, the continuous state pdf at time $k+1$ is given by

  $$\begin{aligned}p[x(k+1)|\mathscr{Z}^{k_c}] = &\sum_{j=1}^{n_d}p[x(k+1)\\ &|q(k+1)=j,\mathscr{Z}^{k_c}]Pr\{q(k+1)=j|\mathscr{Z}^{k_c}\}\end{aligned} \qquad (21)$$

  We approximate the sum of the n_d terms in (21) via moment matching by a single Gaussian pdf:

  $$p[x(k+1)|\mathscr{Z}^{k_c}] \approx \mathscr{N}_n(x;\hat{x}(k+1),P(k+1))$$

where

$$\hat{x}(k+1) = \sum_{j=1}^{n_d} \alpha_j(k+1)\hat{x}_j(k+1|k+1)$$

$$P(k+1) = \sum_{j=1}^{n_d} \{P_j(k+1|k+1) + \alpha_j(k+1)$$
$$[\hat{x}_j(k+1|k+1) - \hat{x}(k)][\hat{x}_j(k+1|k+1) - \hat{x}(k)]^T\}$$

B. Conflict Detection Algorithm

In Section II-B, it has been shown that the conflict detection involves evaluation of the integration in (10). A straightforward approach is to use the Monte Carlo simulation to compute (10) [6], which is computationally expensive. To improve the accuracy and computational efficiency of conflict detection, we propose an algorithm based on the method of *cumulative distribution function (cdf) approximation*. Equation (10) can be rewritten as:

$$\begin{aligned} Pr\{\mathscr{C}(k)\} &= \int_{\rho\in\mathscr{D}} \mathscr{N}_3(\rho;\bar{\rho}_{12}(k);\Sigma_{12}(k))d\rho \\ &= Pr\{\rho_{12}(k)\in\mathscr{D}\} \\ &= Pr\{\kappa(k)\le 1\} \end{aligned} \tag{22}$$

where

$$\kappa(k) = \rho_{12}^T(k)\Psi\rho_{12}(k) \quad \text{and} \quad \Psi = \begin{bmatrix} \frac{1}{s^2} & 0 & 0 \\ 0 & \frac{1}{s^2} & 0 \\ 0 & 0 & \frac{1}{H^2} \end{bmatrix} \tag{23}$$

Consider a general case in which $\Psi\in\mathbb{R}^{M\times M}$ is an indefinite Hermitian matrix (the definite matrix case can be solved in a similar way) and $\omega\in\mathbb{R}^M$ and $p[\omega] = \mathscr{N}_M(\omega;\bar{\omega},\Sigma_\omega)$. The quadratic form is given by:

$$\kappa = \omega^T\Psi\omega \tag{24}$$

Firstly, we look for a orthogonal matrix P^* to diagonalize the Hermitian matrix $\Sigma_\omega^{\frac{1}{2}}\Psi\Sigma_\omega^{\frac{1}{2}}$, such that

$$P^{*T}\Sigma_\omega^{\frac{1}{2}}\Psi\Sigma_\omega^{\frac{1}{2}}P^* = \mathrm{diag}(\lambda_1,\ldots,\lambda_M), P^*P^{*T} = I$$

where $\lambda_1,\ldots,\lambda_M$ are eigenvalues of the matrix $\Sigma_\omega^{\frac{1}{2}}\Psi\Sigma_\omega^{\frac{1}{2}}$. The quadratic form of ω: $\kappa=\omega^T\Psi\omega$ can be rewritten as [12]:

$$\kappa = \sum_{j=1}^{M}\lambda_j(U_j+b_j)^2 \tag{25}$$

where $U_j\sim\mathscr{N}(0,1)$ are mutually independent, and $b^T = [b_1,\ldots,b_M] = (P^{*T}\Sigma_\omega^{-\frac{1}{2}}\bar{\omega})^T$. Let $U=[U_1,\ldots,U_M]^T$. Then, we have $U = P^{*T}\Sigma_\omega^{-\frac{1}{2}}(\omega-\bar{\omega})$. Next, we group the eigenvalues $\lambda_1,\ldots,\lambda_M$ to a set of λ_k, $k=0,\ldots,N-1$, each with multiplicity m_k so that $M=\sum_{k=0}^{N-1}m_k$. We define

$$\mu_k^2 = \sum_{m_k} b_j^2 \tag{26}$$

The computation of the cdf and pdf of the quadratic form (24) involves finding the inverse Laplace transformation of the moment-generating function of (25) [13]:

$$Pr\{\kappa\ge y\} = -\frac{1}{2\pi i}\oint_C \frac{1}{s}e^{-sy}\Phi(s)ds \tag{27}$$

where $y>0$ is any given number; C is a contour encircling the right half plane; and $\Phi(s)$ is the moment-generating function of (25) which can be written as:

$$\Phi(s) = \exp\left\{-\frac{1}{2}\sum_j\mu_j^2 + \frac{1}{2}\sum_j\frac{\mu_j^2}{1-\lambda_j s}\right\}\prod_j\frac{1}{(1-\lambda_j s)^{m_j}} \tag{28}$$

To compute the inverse Laplace transformation of (28), we define

$$g_k(s,y) = \exp\left\{\frac{1}{2}\sum_{j\ne k}\frac{\mu_j^2}{\alpha_{kj}-\lambda_j s} - sy\right\}\prod_j\frac{1}{(\alpha_{kj}-\lambda_j s)^{m_{kj}}} \tag{29}$$

for each λ_k with multiplicity m_k. Note that in (29), we define $\alpha_{kj} = 1-\lambda_j/\lambda_k$, $m_{kj}=m_j$ for $j\ne k$, and $\alpha_{kk}=-1$, $m_{kk}=1$ for $j=k$. Next, we need to compute recursively the derivatives of g_k up to the n-th order. Note that

$$\ln g_k(s,y) = \frac{1}{2}\sum_{j\ne k}\frac{\mu_j^2}{\alpha_{kj}-\lambda_j s} + \sum_{j\ne k}m_j\ln\left(\frac{1}{\alpha_{kj}-\lambda_j s}\right) - sy \tag{30}$$

By induction, we have

$$[\ln g_k(s,y)]^{(n)} = \frac{1}{2}\sum_{j\ne k}\frac{n!\lambda_j^n\mu_j^2}{(\alpha_{kj}-\lambda_j s)^{n+1}} + \sum_{j\ne k}\frac{(n-1)!\lambda_j^n m_j}{(\alpha_{kj}-\lambda_j s)^n} \tag{31}$$

Taking $(n-1)$-th derivative of both sides of $g_k^{(1)} = g_k(\ln g_k)^{(1)}$, we have [12]:

$$g_k^{(n)} = \sum_{l=0}^{n-1}\binom{n-1}{l}g_k^{(l)}(\ln g_k)^{(n-l)}, \quad n\ge 1 \tag{32}$$

By using (32), for a given $g_k^{(0)}(0,y)$, we can compute $g_k^{(n)}(0,y)$ recursively. Next we define $\beta_k = \mu_k^2/(2\lambda_k)$. We can compute the probability (25) based on the Laurent series and the Taylor series expansion:

$$\begin{aligned} Pr\{\kappa\le y\} = 1 - \exp\left\{-\frac{1}{2}\sum_j\mu_j^2\right\}\sum_{\lambda_k>0}\Bigg\{\frac{1}{(-\lambda_k)^{m_k-1}} \\ \exp(-\lambda_k^{-1}y)\sum_{n=m_k-1}^{\infty}\hat{g}_k^{(n)}(0,y)\frac{(-\beta_k)^{(n-m_k+1)}}{n!(n-m_k+1)!}\Bigg\} \end{aligned} \tag{33}$$

In (33), letting $y=1$ and taking finite terms in the third summation, we can evaluate (33) and (22).

IV. SIMULATIONS

In the simulation, Aircraft 1 (a_1) starts from Point A heading towards the north, while Aircraft 2 (a_2) starts from Point B heading towards the east (see also Figure 1). Both aircraft are flying straight at the initial stage. Since the altitude difference between them is bigger than the minimum vertical separation distance ($1000ft$), there is no potential conflict initially. However, to avoid the adverse weather cell $\mathscr{W}$, Aircraft 2 climbs to the same altitude as Aircraft 1, which generates a potential conflict.

Next, we present the discrete-time continuous dynamics of both aircraft in the (ξ, η, h) frame. The state vector of

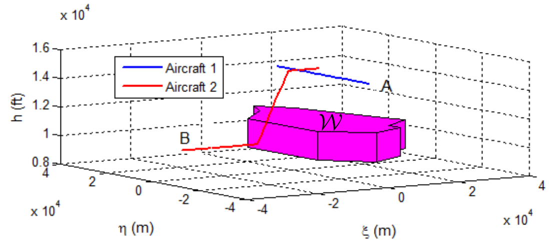

Fig. 1. Two-aircraft conflict scenario.

each aircraft is $x = \begin{bmatrix} \xi & \dot{\xi} & \eta & \dot{\eta} & h \end{bmatrix}^T \in \mathscr{X} = \mathbb{R}^5$. The aircraft dynamics in the horizontal plane is given by:

$$x(k+1) = Ax(k) + Bw(k) \tag{34}$$

where

$$A = \begin{bmatrix} 1 & T_s & 0 & 0 \\ 0 & 1 & 0 & 0 \\ 0 & 0 & 1 & T_s \\ 0 & 0 & 0 & 1 \end{bmatrix} \qquad B = \begin{bmatrix} \frac{T_s^2}{2}\omega_{\xi 1} & 0 \\ T_s\omega_{\xi 1} & 0 \\ 0 & \frac{T_s^2}{2}\omega_{\eta 1} \\ 0 & T_s\omega_{\eta 1} \end{bmatrix}$$

and $w(k) \in \mathbb{R}^2$ is a standard white Gaussian noise vector; $T_s = 5sec$ is the sampling time; and $\omega_{\xi 1} = \omega_{\eta 1} = 0.5m/s^2$ are scaling parameters [9].

The aircraft motion in the vertical dimension consists of two modes: Mode 1: Constant Height (CH), and Mode 2: Constant Climb (CC). Therefore, $\mathscr{Q} = \{1, 2\}$. The continuous dynamics of the CH mode is given by:

$$h(k+1) = h(k) + T_s w_{CH}(k) \tag{35}$$

where $w_{CH}(k) \in \mathbb{R}$ is a standard Gaussian noise vector. The continuous dynamics of the CC mode is given by:

$$h(k+1) = h(k) + T_s w_{CC}(k) + u \tag{36}$$

where $w_{CC}(k) \in \mathbb{R}$ is a standard Gaussian noise vector; and $u = 30m/s$ is a constant input which specifies the aircraft's climbing rate.

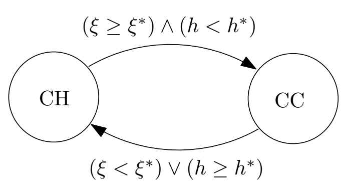

Fig. 2. Aircraft discrete state transition model (Note that we use "$\wedge$" to denote logical "AND" and "$\vee$" to denote logical "OR").

The discrete state transition model is shown in Figure 2. The transition can be described as follows: Aircraft 2 is originally in the CH mode; when it is close to the adverse weather cell, it pulls up and enters the CC mode; after it reaches a new altitude which allows it to pass the weather cell safely, Aircraft 2 enters the CH mode again. To model the uncertainties in these transitions, we use two Gaussian random variables $\xi^* \sim \mathscr{N}(\bar{\xi}^*, \Sigma_{\xi^*}) \in \Xi = \mathbb{R}$ and $h^* \sim \mathscr{N}(\bar{h}^*, \Sigma_{h^*}) \in \mathscr{H} = \mathbb{R}$ to denote the thresholds for the transitions. In the simulation, we choose $\bar{\xi}^* = -1 \times 10^4 m$, $\Sigma_{\xi^*} = 3 \times 10^3 m$, $\bar{h}^* = 1.45 \times 10^4 ft$ and $\Sigma_{h^*} = 700 ft$. Thus, the guard conditions defined in the space $\Omega = \{\mathscr{X} \times \Xi \times \mathscr{H}\} = \mathbb{R}^7$are given by:

$$\begin{aligned} G(1,2) =& \{[x\ \xi^* h^*]^T \,|x \in \mathscr{X}, \xi^* \in \Xi, h^* \in \mathscr{H}, \\ & (\xi \geq \xi^*) \wedge (h < h^*)\} \\ G(1,1) =& \Omega \backslash G(1,2) \\ G(2,1) =& \{[x\ \xi^* h^*]^T \,|x \in \mathscr{X}, \xi^* \in \Xi, h^* \in \mathscr{H}, \\ & (\xi < \xi^*) \vee (h \geq h^*)\} \\ G(2,2) =& \Omega \backslash G(2,1) \end{aligned}$$

A simulation of the total length $250sec$ is performed. The transition from Mode 1 to Mode 2 happens around $125sec$ and the transition from Mode 2 back to Mode 1 happens around $175sec$. Our trajectory prediction starts from $110sec$ and the prediction time horizon is $120sec$ ($2min$). Before we begin the prediction, the hybrid state estimates are computed by the standard IMM algorithm with the aircraft position information provided by radar in every $5sec$.

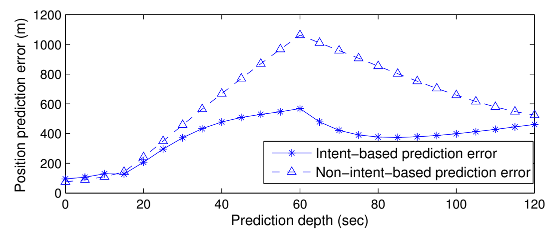

Fig. 3. Aircraft 2's position prediction error (RMS error of 100 Monte Carlo run).

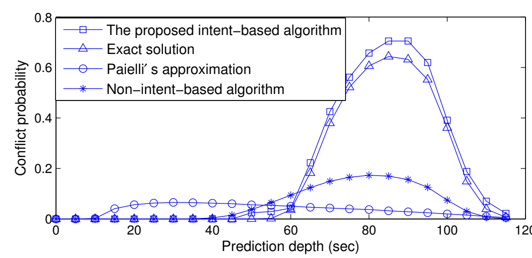

Fig. 4. Comparison of conflict probabilities computed by different algorithms.

Figure 5 shows the trajectory prediction results of the intent-based algorithm and the non-intent-based algorithm in the 3-D space. The red bulbs are the σ ellipsoids of the Gaussian random variables representing the uncertainties of each prediction result. From Figure 5, we can deduce that the intent-based algorithm yields prediction results with lower uncertainties, because the intent-based algorithm accurately predicts the true flight mode utilizing the prior information about when and where the flight mode transition is supposed to happen. On the other hand, the non-intent-based algorithm assumes a constant Markov transition matrix for the flight mode transition. Through a Monte Carlo simulation of 100

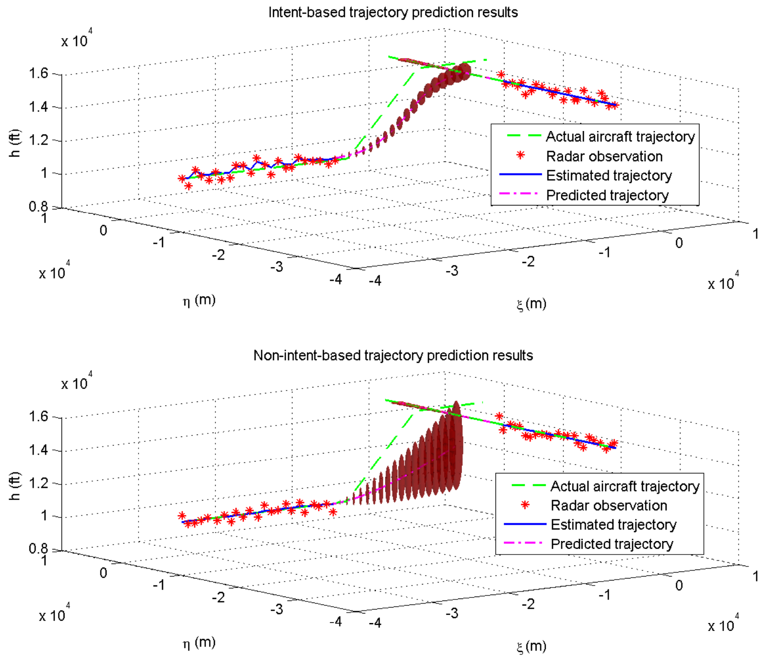

Fig. 5. Aircraft trajectory prediction results.

runs, Figure 3 compares the Root-Mean-Square (RMS) trajectory prediction errors of Aircraft 2 with the intent-based and the non-intent-based algorithms.

Figure 4 compares the conflict probabilities computed by four different algorithms: the proposed cdf approximation algorithm yields the result that is the closest to the exact solution computed by the Monte Carlo approach. The non-intent-based algorithm and the Paielli's algorithm [5] show poor conflict probability estimation due to their over-approximation. Additionally, our algorithm is much more computationally efficient than the Monte Carlo approach in calculating the integration (22) [14].

V. CONCLUSIONS

We have developed a computationally efficient algorithm for aircraft trajectory prediction and conflict detection. We use the Stochastic Linear Hybrid System (SLHS) to model the dynamics of an aircraft with changing flight modes and compute the accurate prediction of an aircraft's future trajectory efficiently. To estimate the conflict probability accurately and efficiently, we use the cumulative distribution function (cdf) approximation.

VI. ACKNOWLEDGEMENT

The authors would like to acknowledge that this work is supported by NSF CAREER Award CNS-0746299 and to thank Dr. Helen Gill for her support.

REFERENCES

[1] Concept of operations for the next generation air transportation system. Technical report, Joint Planning and Development Office, Febrauary 2007.

[2] I. Hwang and C.E. Seah. Intent-based probabilistic conflict detection for the next generation air transportation system. *Proceedings of the IEEE*, 96(12):2040–2059, Dec. 2008.

[3] J.K. Kuchar and L.C. Yang. A review of conflict detection and resolution modeling methods. *IEEE Transactions on Intelligent Transportation Systems*, 1(4):178–189, December 2000.

[4] J. Lygeros and M. Prandini. Aircraft and weather models for probabilistic collision avoidance in air traffic control. In *Proceedings of the 41st IEEE Conference on Decision and Control, Las Vegas*, pages 2427–2432, 2002.

[5] R.A. Paielli and H. Erzberger. Conflict probability estimation for free flight. *Journal of Guidance, Control and Dynamics*, 20(3):588–596, 1997.

[6] L.C. Yang and J.K. Kuchar. Using intent information in probabilistic conflict analysis. In *Proceedings of AIAA Guidance, Navigation, and Control Conference 1998*, pages 797–806, Boston, MA, August 1998.

[7] J. Hu, M. Prandini, and S. Sastry. Aircraft conflict prediction in the presence of a spatially correlated wind field. *IEEE Transactions on Intelligent Transportation Systems*, 6(3):326–340, Sept. 2005.

[8] Y. Bar-Shalom, X. R. Li, and T. Kirubarajan. *Estimation with Applications to Tracking and Navigation*. John Wiley & Sons, 2001.

[9] C. E. Seah and I. Hwang. Stochastic linear hybrid systems, modeling, estimation, and application in air traffic control. *IEEE Transactions on Control Systems Technology*, 2008. accepted.

[10] M. Prandini, J. Hu, J. Lygeros, and S. Sastry. A probablistic approach to aircraft conflict detection. *IEEE Transactions on Intelligent Transportation Systems*, 1(4):199–220, December 2000.

[11] H.A.P. Blom and Y. Bar-Shalom. The interacting multiple model algorithm for systems with Markovian switching coefficients. *IEEE Transactions on Automatic Control*, 33(8):780–783, 1988.

[12] A. M. Mathai and S. B. Provost. *Quadratic Forms in Random Variables: Theory and Applications*, volume 126. Marcel Dekker, Inc., New York, 1992.

[13] G. L. Turin. The characteristic function of hermitian quadratic forms in complex normal variables. *Biometrika*, 47:199–201, 1960.

[14] C.E. Seah W. Liu and I. Hwang. Estimation algorithm for stochastic linear hybrid systems with quadratic guard conditions. In *Proceedings of the 48th IEEE Conference on Decision and Control*, Shanghai, China, Dec 2009.